Probing Matter Radii of Neutron-Rich Nuclei by Antiproton Scattering

Horst Lenske[1] and Paul Kienle[2]
[1] *Institut für Theoretische Physik, Universität Gießen, Heinrich-Buff-Ring 16, D-35392 Gießen, Germany*
[2] *Fakultät für Physik, Technische Universität München, James Franck Str. 1, D-85748 Garching, Germany, and Stefan Meyer Institut für subatomare Physik, Boltzmanngasse 3, A-1090 Wien, Austria*
(Dated: February 9, 2008)

We propose to use antiprotons to investigate the sizes of stable and neutron-rich exotic nuclei by measurements of the $\overline{p}A$ absorption cross section along isotopic chains in inverse kinematics. The expected effects are studied theoretically in a microscopic model. The $\overline{p}U$ optical potentials are obtained by folding free space $\overline{p}N$ scattering amplitudes with HFB ground state densities and solving the scattering equations by direct integration. The mass dependence of absorption cross sections is found to follow closely the nuclear root-mean-square radii. The total absorption cross section is shown to be a superposition of cross sections describing partial absorption on neutrons and protons, respectively. Thus measuring the differential cross sections for absorption on neutrons and protons will give information on their respective distributions. In neutron-rich nuclei the outer neutron layer shields the absorption on the protons giving access to investigations of antiproton-neutron interactions in matter.

PACS numbers: 21.10.Gv,21.60.Jz,25.43.+t,25.60.Bx
Keywords: antiproton, exotic nuclei, nuclear sizes

I. INTRODUCTION

To understand the evolution of nuclear sizes and shapes from the bottom to the edges of the valley of $\beta-$ stability is one of the central questions of modern nuclear structure physics. Experimentally, a variety of efforts is undertaken or in planning to investigate properties of neutron-rich exotic nuclei ranging from high-energy breakup reactions [1] and elastic proton scattering [2] to charge-exchange reactions [3] and low-energy transfer reactions [4, 5]. Here, we propose to use antiprotons to probe nuclear sizes of stable and unstable nuclei in a systematic way.

Investigations of radii and density distributions of stable nuclei by antiprotons are by itself a long discussed and applied method, e.g. at BNL [6, 7] or LEAR [8, 9, 10, 11]. Hitherto, the experiments have been performed with secondary antiproton beams on a variety of stable nuclei in fixed target geometry and standard kinematics, actually using stopped antiprotons. Obviously, another approach must be applied if antiprotons should be used for reactions on short-lived isotopes. These nuclei by themselves are available also only as secondary beams, produced either by fragmentation or isotope separation on line. A solution dissolving these conflicting conditions is to perform the measurements in colliding beam geometry. Such a setup was recently proposed in [12]. It will become feasible with the meanwhile approved FAIR facility a GSI [14]. The FAIR plans include as central components $\overline{p}$ production and accumulation facilities. For nuclear structure research the New Experimental Storage Ring (NESR) for short-lived nuclides and an intersecting electron accelerator for colliding beam experiments will be available [13]. As discussed in the Antiproton-Ion-Collider (AIC) proposal [15], with moderate modifications on an acceptable level the NESR/e^- setup can be converted into a $\overline{p}A$ collider facility. Details of the experimental setup and procedures for the measurement of antiproton absorption cross sections using Schottky noise frequency spectroscopy of the coasting reaction products in the NESR are found in the NUSTAR letter of intent and proposal for FAIR [12, 16].

The physics of $\overline{p}A$ interactions is by itself an interesting topic for nuclear and hadron physics. It was brought to the attention of nuclear physics originally by Duerr and Teller [17]. The usefulness of $\overline{p}+A$ scattering for studies of the neutron skin in stable medium and heavy nuclei was realized some years later in an experiment at BNL [6]. In the aftermath, a variety of experiments have been performed, e.g. [8, 9, 10, 11]. As for the elementary antiproton nucleon ($\overline{p}N$) vertex the $\overline{p}A$ reactions are dominated by processes in which the incoming antiproton annihilates on a target nucleon into a variety of particles producing typically and preferentially a shower of pions as the final result. Here, we utilize the strong $\overline{p}A$ absorption for nuclear structure investigations without paying particular attention to the hadron physics aspects, some of which, however, can – and in another context will – be studied with the facility under discussion, e.g. with the PANDA detector, also being part of the FAIR proposal.

For our purpose we are satisfied to know that the elementary annihilation processes result finally in a strong suppression of the incoming flux. In the elementary elastic scattering amplitude $f_{\overline{p}N}$ the annihilation channels appear as a strong imaginary part while only a small, almost vanishing, real part is observed. Correspondingly, in potential models for inclusive $\overline{p}A$ elastic scattering the annihilation channels are typically accounted for globally by a strongly

absorptive optical potential, as e.g. in [20, 21, 22, 23]. In fact, the total cross section is about twice the elastic cross section [24] which underlines the importance of the annihilation channels.

The new aspect of the present paper is to explore theoretically the perspectives of antiproton scattering on stable and rare nuclei and the use of such reactions for nuclear structure investigations. In particular, we consider elastic $\overline{p}A$ scattering and study to what degree the total reaction or absorption cross section provides information on the size and shape of the target nucleus. The theoretical approach is described in sect. II. As a typical and interesting case absorption cross sections for the Ni isotopic chain are discussed in sect.II B. The paper closes with a summary in sect.III.

II. MICROSCOPIC DESCRIPTION OF ANTIPROTON ABSORPTION ON NUCLEI

A. Optical Model Approach for $\overline{p}A$ Elastic Scattering

The basic ingredients for a microscopic description of $\overline{p}A$ scattering are obviously the elementary antiproton-nucleon interactions. Including a spin-independent amplitude $A(\sqrt{s},t)$ and a spin-orbit part $C(\sqrt{s},t)$ the free space antiproton scattering amplitude is taken to be

$$f_{\overline{p}N}(\sqrt{s},q) = A(\sqrt{s},t) + C(\sqrt{s},t)\frac{1}{k}\sigma_{\overline{p}}\cdot(\mathbf{q}\times\mathbf{k}) \quad , \tag{1}$$

where k is the momentum of the incoming antiproton, s the Mandelstam center of mass energy and $q^2 = -t$ is the momentum transfer. For kinetic energies $\mathrm{T}_{lab} \lesssim 1500$ MeV the data clearly show that the $\overline{p}N$ interactions are dominated by annihilation processes. By means of the optical theorem an effective T-matrix is defined

$$t_{\overline{p}N}(T_{Lab},q^2) = \frac{2\pi\hbar}{M}\frac{ik}{4\pi}\sigma_{\overline{p}N}(T_{Lab})\,(1-i\epsilon)\,F_{\overline{p}N}(q^2) \tag{2}$$

where $T_{Lab} = E_{Lab}(k) - M$ is the kinetic energy of the incoming antiproton with momentum k and the total $\overline{p}N$ cross section $\sigma_{\overline{p}N}(T_{Lab})$. The ratio of the real and the imaginary part is denoted by ϵ which lies between $\frac{1}{4}\cdots\frac{1}{3}$ in the energy range considered here. As in [25] we use a t-channel form factor of gaussian shape, $F(q^2) \equiv e^{-\beta^2 q^2}$. A closer inspection shows that by eq.2 $t_{\overline{p}N}$ is assumed to be separable into an on-shell strength factor and an off-shell form factor.

The coordinate space $\overline{p}A$ optical potential is then obtained in the *impulse* approximation and after a Fourier transformation,

$$U_{opt}(\mathbf{r}) = \sum_{N=p,n}\int\frac{d^3q}{2\pi^3}\rho_N(q)t_{\overline{p}N}(T_{Lab},q^2)e^{i\mathbf{q}\cdot\mathbf{r}} \quad , \tag{3}$$

a strongly absorptive complex optical potential $U_{opt} = V + iW$ with real and imaginary parts V and W, respectively, is obtained. Obviously, we have $U_{opt} = U_{opt}^{(p)} + U_{opt}^{(n)}$.

In practice, we use the momentum space amplitudes, including also a complex spin-orbit part, derived in [25] according to the Paris model [27]. As in the elementary $\overline{p}N$ interaction the potentials are dominated by strong imaginary parts. We also include the (long range) Coulomb potential U_c which is calculated microscopically by folding the elementary $\overline{p}N$ Coulomb amplitude with the HFB charge density ρ_c. The elementary proton and neutron electric form factors $G_E^{(n,p)}(q^2)$ are taken into account. The $\overline{p}A$ spin-orbit optical potentials U_{so} are calculated with the HFB spin densities. Although the resulting U_{so} are rather weak and, in particular, do not contribute significantly to the absorption they are taken into account in the calculations for completeness.

We use a non-relativistic approach and describe $\overline{p}A$ scattering by the optical model Schroedinger equation

$$\left(-\frac{\hbar^2}{2\widetilde{m}}\overrightarrow{\nabla}^2 + U_{opt} - T_{cm}\right)\Psi_\alpha^{(+)}(\mathbf{k},\mathbf{r}) = 0 \quad . \tag{4}$$

Here, $\Psi_\alpha^{(+)}(\mathbf{k},\mathbf{r})$ is the optical model wave function for the incoming proton in spin state $m_\alpha = \pm\frac{1}{2}$ and with asymptotically outgoing spherical waves. The antiproton-nucleus center-of-mass system with reduced mass $\widetilde{m}$ is used.

From the solutions of eq.4 we determine the partial wave S-matrix elements $S_{\ell j}$ [28] where for an absorptive system $|S_{\ell j}| < 1$. The continuity equation for the optical model wave function $\Psi^{(+)}$ provides us with the exact relation

$$\sigma_{abs} = \frac{\pi}{k^2}\sum_{\ell j}\frac{2j+1}{2s+1}(1-|S_{\ell j}|^2) = -\frac{2\widetilde{m}}{k\hbar^2}\frac{1}{2s+1}tr_s\left(\int d^3r\Psi^{(+)\dagger}(\mathbf{k},\mathbf{r})\Im(U_{opt})(\mathbf{r})\Psi^{(+)}(\mathbf{k},\mathbf{r})\right) \quad , \tag{5}$$

with averaging over the $\overline{p}$ spin projections. The second equality provides us with a particular useful relation: From eq.3 we know $\Im(U_{opt}) = W_p + W_n$ which immediately implies additivity for $\sigma_{abs} = \sigma_{abs}^{(p)} + \sigma_{abs}^{(n)}$ and the partial cross section for annihilation on $q = p, n$, respectively, are given by

$$\sigma_{abs}^{(q)} = -\frac{2\widetilde{m}}{k\hbar^2}\frac{1}{2s+1} tr_s \left(\int d^3r |\Psi^{(+)\dagger}(\mathbf{k},\mathbf{r})|^2 W_q(\mathbf{r}) \right) \quad . \tag{6}$$

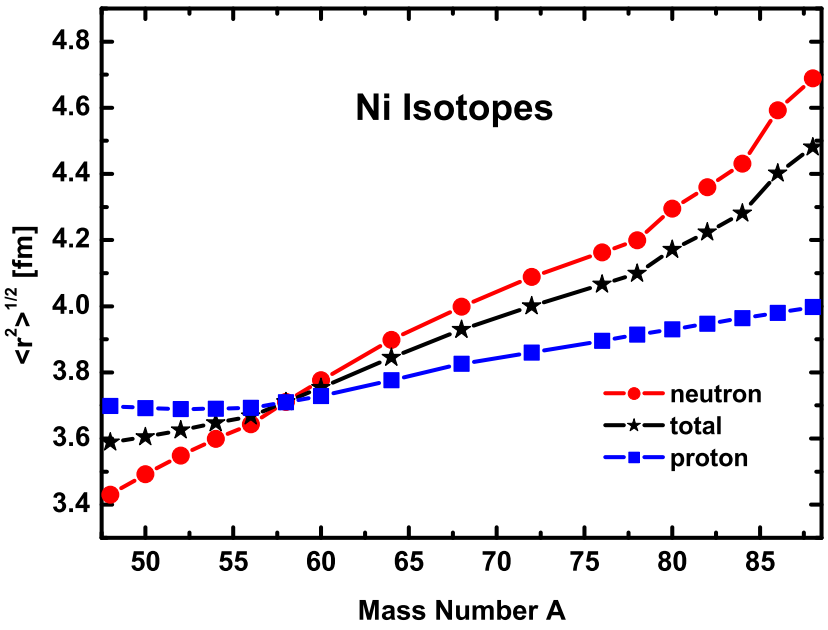

FIG. 1: Root-mean-square (rms) radii for $^{48-88}$Ni-isotopes. HFB results for protons (squares), neutrons (circles) and the total (isoscalar) density (stars) are shown. The mass range corresponds to the isotopes found in the HFB calculations to be particle-stable. The lines are to guide the eye. Note the change from proton skins at $A \lesssim 58$ to neutron skins at larger mass numbers.

For our aim eq.6 is of particular interest because the leading order proton and neutron contributions to σ_{abs} are being displayed explicitly. Hence, we have succeeded to represent the annihilation on the target protons and neutrons in a formally separable form allowing to study theoretically the corresponding partial absorption cross sections separately. However, we note that in eq.6 the distorted waves are determined by U_{opt} in a non-perturbative manner and, as such, include the whole multitude of effects from $W_{p,n}$.

The ground state densities entering into the optical potentials are taken from non-relativistic HFB calculations using a G-Matrix interaction as described in [29]. The known deficiencies of non-relativistic Brueckner-calculations are overcome by introducing additional density dependent contributions [29, 31] and adjusting the parameters to the variational results for infinite nuclear matter of the Urbana group [30]. An effective density dependent zero-range pairing interaction is derived from the SE (S=0,T=1) in-medium NN-interaction [31]. The system of coupled state dependent HFB gap equations is solved self-consistently. HFB results for rms-radii of the proton and neutron ground state densities in the Ni isotopes are displayed in Fig.1. We also find a very satisfactory overall agreement of the theoretical and the measured binding energies on the level of 5%, see e.g. [31, 32]

B. Absorption Cross Sections for $\overline{p}$ Annihilation on the Ni-Isotopes

While for most $\overline{p}A$ investigations the strong absorption is an unwanted and disturbing effect, we take advantage of this property: Because of the strong absorption the product of scattering waves in eq.6 gains strength mainly

in the nuclear surface thus favoring investigations of nuclear skin configurations. As seen from eq.6 this behavior, common for both the proton and neutron partial cross sections, is modulated by the specific shape of $W_{p,n}$ leading to a pronounced weighting of the nuclear surface region. Thus, measurements of the $\overline{p}A$ absorption cross section will provide us with data proving the existence of nuclear skins and recording their properties like their composition and mass dependence.

The total absorption cross sections for Ni-Isotopes in the mass range 48≤A≤88 are shown in Fig.2. Results for antiproton incident energies from T_{Lab} =50 MeV to T_{Lab} =400 MeV are displayed. With increasing energy the magnitude of σ_{abs} decreases at a rate slowing down when approaching the highest shown energy, T_{lab} = 400 MeV. A remarkable feature common to all energies is the steady increase with mass number, reflecting the growth of the neutron skin with the neutron excess.

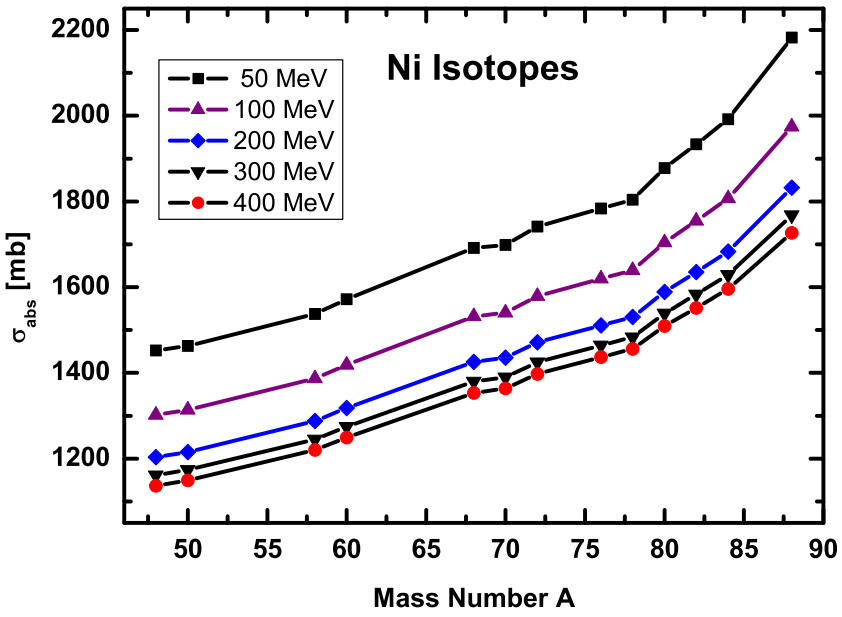

FIG. 2: Absorption cross sections for antiproton annihilation on the $^{48-88}$Ni-isotopes at various antiproton incident energies. The lines are to guide the eye.

In Fig.3 the absorption cross sections at T_{Lab}=200 MeV and T_{Lab}=400 MeV are compared to the rms-radii of the nuclear ground state number density distributions. At both energies the nuclear rms-radii were normalized arbitrarily to the cross sections at ^{58}Ni expressed by the scaling law $\sigma_{abs} \simeq \alpha_0 \langle r^2 \rangle$. From Fig.3 we note an impressive agreement for σ_{abs} and the rms radii, both increasing with almost the same slope as functions of the target mass. This behavior is found at all energies considered here, thus indicating an almost universal scaling law . The normalization constants α_0 are slowly varying with the incident energy, decreasing by about 5% from T_{Lab} = 200 MeV to T_{Lab} = 400 MeV. Their origin and physical content will be discussed below. We conclude that antiproton annihilation is a well suited probe for investigating nuclear sizes and shapes.

It is instructive to inspect $\overline{p}A$ scattering along a trajectory through the target nucleus by means of the eikonal approximation [28]. The partial absorption cross sections for $q = p, n$ at impact parameter b are given by

$$\sigma_{abs}^{(q)}(b) = \frac{2\pi}{k}\frac{\widetilde{m}}{\hbar^2}\int_{-\infty}^{+\infty} dz \Pi_q(z,b) \quad , \tag{7}$$

with the eikonal absorption kernel

$$\Pi_q(z,b) = \frac{1}{2s+1} tr_s\{\Pi^{(s)}(z,b)\} = -e^{-2\chi_q(z,b)} W_q(z,b) \quad , \tag{8}$$

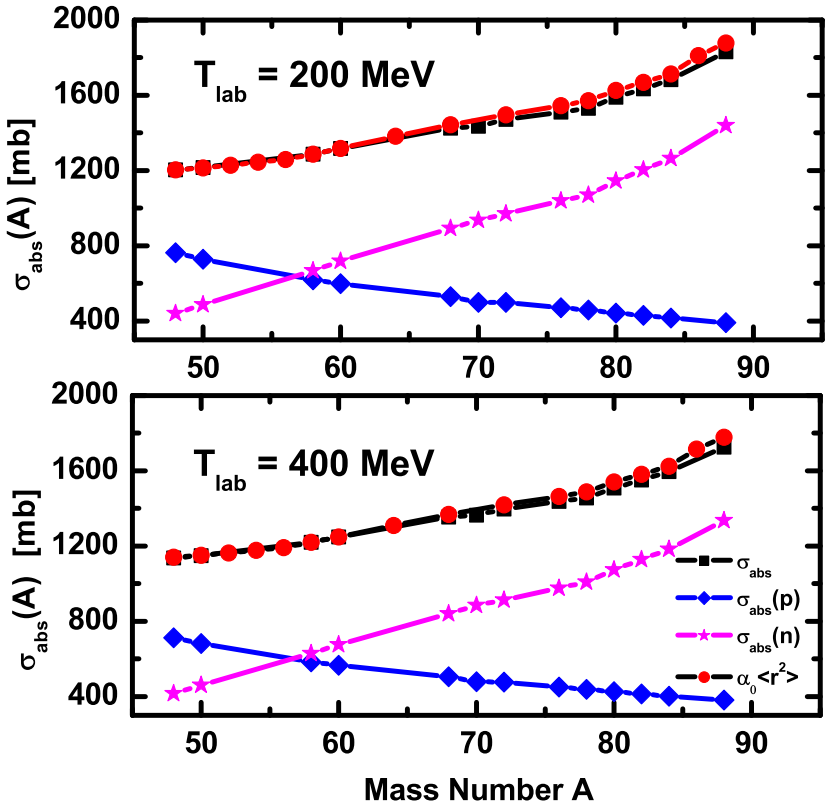

FIG. 3: Absorption cross sections (filled squares) for antiproton annihilation on Ni-isotopes at $T_{lab} = 200$ MeV and $T_{lab} = 400$ MeV, respectively, are compared to the rms-radii of the nuclear matter densities (filled circles). In both cases, the rms-radii are arbitrarily normalized by a factor α_0 to σ_{abs} for ^{58}Ni. Also shown are the partial cross sections for absorption on the target neutrons (stars) and protons (diamonds).

including a trace over spin projections. The eikonal integral

$$\chi_q(z,b) = -\frac{2\widetilde{m}}{k\hbar^2}\int_{-\infty}^{z} d\xi W_q(\xi,b) \tag{9}$$

describes the depletion of the incoming antiproton flux along the trajectory through the target nucleus. These relations show that $\Pi(z,b)$ is a measure for the degree of absorption at a given point in the (z,b) scattering plane. Overall, for impact parameters b less than the target radius R_A the incoming flux is strongly absorbed, giving the target the characteristics of a black disk.

In Fig.4, results for $\Pi(z,b)$ are displayed at $T_{Lab} = 300$ MeV for a variety of Ni nuclei and an impact parameter $b = 4$ fm which roughly corresponds to grazing collisions over the mass region considered in Fig.4. We find an interesting mass dependence: In the neutron-deficient ^{48}Ni the absorption is takes place dominantly in the **proton skin** and with increasing neutron number the process changes gradually to absorption on the neutrons with a break-even point around ^{58}Ni. In the extremely neutron-rich isotopes beyond ^{78}Ni the antiprotons are absorbed preferentially in the neutron skin, i.e. in the outer layers of the nuclear density distribution. As a consequence, in the neutron-rich isotopes the more tightly bound and spatially more confined protons are effectively screened from the incoming $\overline{p}$ flux by the neutron skin. This implies that the antiprotons are preferentially annihilated in a region of almost pure neutron matter. The screening effect also explains the decrease of the partial proton and the increase of the partial neutron optical model cross sections,respectively, seen in Fig.3. In fact, the eikonal approach leads to a very satisfying agreement with the exact optical model results even on the quantitative level. Above $T_{Lab} \simeq 100$ MeV both descriptions agree by better than 10% and, as to be expected, the deviations diminish with increasing incident energy.

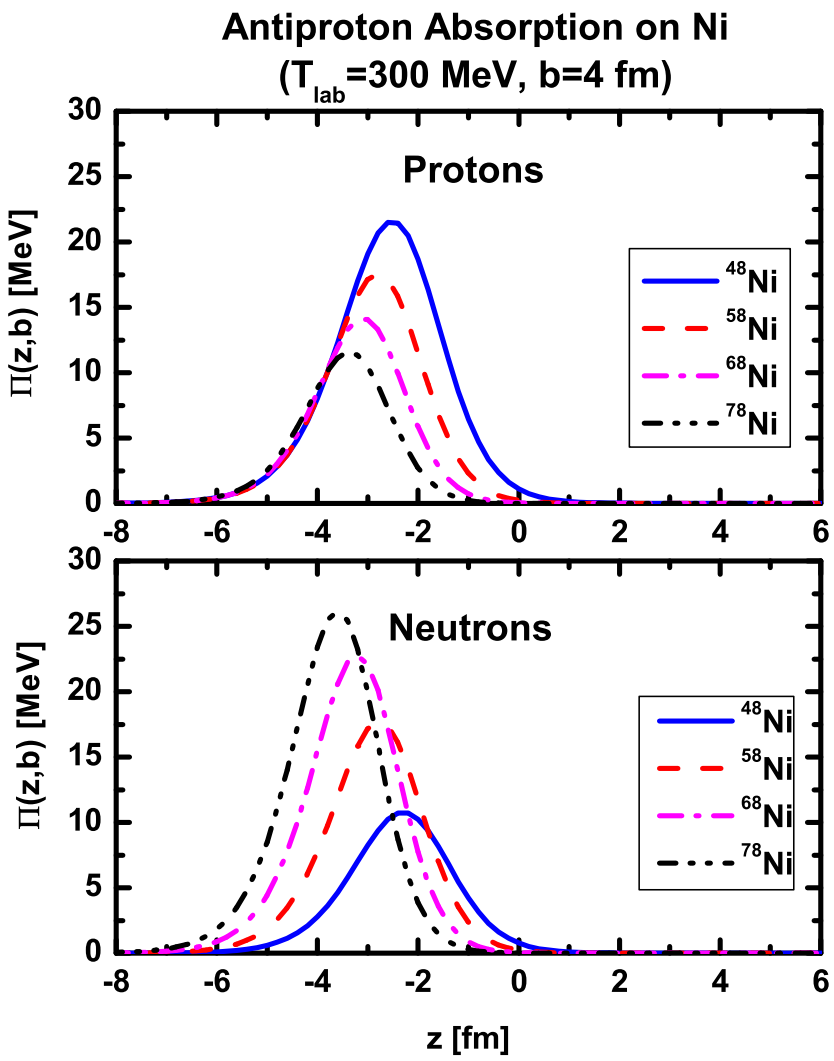

FIG. 4: Absorption of the incoming antiproton flux along a trajectory with impact parameter $b = 4$ fm. The eikonal absorption kernel, eq.8, is displayed for annihilation of antiprotons with an incident energy of $T_{lab} = 300$ MeV on ^{48,58,68,78}Ni. The $\overline{p}$ beam is incoming from the left, i.e. from $z = -\infty$. Note the reversed behavior of the $\overline{p}$ absorption on protons and neutrons with increasing neutron excess.

Assuming a gaussian form factor for $W(r)$ the eikonal cross section, eq.7, can be calculated in closed form, resulting in $\sigma_{abs}(A, T_{cm}) = f(A, T_{cm})\pi\langle r^2\rangle_A$. The eikonal scaling function

$$f(A, T_{cm}) = \gamma + \log\left(\xi(A, T_{cm})\right) + Ei(\xi(A, T_{cm})) \tag{10}$$

describes the deviation from the black disk limit $\sigma_{abs} \to \pi\langle r^2\rangle_A$. $\gamma = 0.5772\cdots$ denotes Euler's constant, $Ei(x)$ is the exponential integral [34] and

$$\xi(A, T_{cm}) = \frac{\sqrt{\pi}\ell_g \Im(t_{\overline{p}N}(T_{cm}))\rho_0}{T_{cm}} \quad . \tag{11}$$

is given in terms of physical quantities, including the $\overline{p}N$ T-matrix, the central nuclear density ρ_0 and $\ell_g = kR_A$ corresponding to the $\overline{p}A$ grazing angular momentum. For the physically relevant values of ξ the $Ei(\xi)$ term can safely be neglected. These relations enable us to interpret in physical terms the scaling factor introduced above. By

comparison we find $\alpha_0 \simeq a_0 = \frac{3\pi}{2} f(A = 58, T_{cm})$. Indeed, approximating the microscopic $W(r)$ by a Gaussian of the same volume integral and rms-radius the analytic eikonal results agree with the full optical model α_0 convincingly well, e.g. $\alpha_0/a_0 \simeq 0.92 \cdots 0.94$ for $T_{Lab} = 100 \cdots 400$ MeV and unity is approached a higher energies. The functional structure of the eikonal scaling factor, eq.10, also explains the apparent convergence of the absorption cross sections to limiting asymptotic values as indicated in Fig.2 for the larger energies. Thus, $f(A, T_{cm})$ and correspondingly α_0 contain valuable information on the dynamics of the $\overline{p}A$ system.

III. CONCLUSIONS AND OUTLOOK

Antiproton-nucleus scattering was investigated theoretically as a tool for measuring neutron skins in exotic nuclei. The $\overline{p}A$ absorption cross sections were calculated with microscopic optical potentials derived from the elementary free space $\overline{p}N$ scattering amplitudes and HFB density distributions. The results point to promising perspectives in at least two directions, namely

- showing that antiprotons are a perfect probe for investigations of neutron (and proton) skins;
- indicating a new method for investigating antiproton-neutron interactions.

The latter point is of particular interest because the data base on $\overline{p}n$ interaction is very scarce. It also adds a new aspect to the experiment proposed in [12, 15]: Scanning over an isotopic chain will allow to record the gradual change from $\overline{p}p$ to $\overline{p}n$ annihilation, hence providing a new access to the *pbar*-nucleon interactions.

Our results show that simple absorption cross section measurements will already provide valuable new information on the densities of the target nuclei, most likely of a higher accuracy than achievable by other methods. More involved measurements seem to be feasible from which more detailed information on the configurations of the target nuclei can be obtained.

A next step will be to consider more exclusive experiments. Differential measurements by gating on the $A-1$ residual nuclei which will provide information on the annihilation of the incoming $\overline{p}$ on a single target neutron or proton, respectively, are being explored [15]. Parallel to the nuclear structure studies the experimental program should also envision investigations of elastic $\overline{p}A$ scattering. A consistent and much extended set of elastic angular distributions is highly desired by theory for a better understanding of antiproton interactions in nuclear matter.

Supported in part by DFG, contract Le 439/05, GSI and BMBF.

[1] D. Cortina-Gil, J. Fernandez-Vazquez, F. Attallah, T. Baumann, J. Benlliure, M.J.G. Borge, L. Chulkov, C. Forssen, L.M. Fraile, H. Geissel, J. Gerl, K. Itahashi, R. Janik, B. Jonson, S. Karlsson, H. Lenske, S. Mandal, K. Markenroth, M. Meister, M. Mocko, G. Münzenberg, T. Ohtsubo, A. Ozawak, Yu. Parfenova, V. Pribora, A. Richter, K. Riisager, R. Schneider, H. Scheit, G. Schrieder, N. Shulgina, H. Simon, A. Sitar, B. Stolz, P. Strmen, K. Sümmerer, I. Szarka, S.Wan, H.Weick M.V. Zhukov, Nucl.Phys. A718 (2003) 431.

[2] P. Egelhof, Nucl. Phys. A22 (2003) C254; G. D. Alkhazov, A. V. Dobrovolsky, P. Egelhof, H. Geissel, H. Irnich, A. V. Khanzadeev, G. A. Korolev, A. A. Lobodenko, G. Mnzenberg, M. Mutterer et al., Nucl.Phys. A712 (2002) 269.

[3] A. Krasznahorkay et al., Phys. Rev. Lett. **82** (1999) 3216; A. Krasznahorkay et al., Proc. of the INPC 2001, Berkeley, Aug. 2001, ed. by E. Norman et al., p.751 (2001).

[4] H. Lenske, G. Schrieder, Eur.Phys.J. **A2** (1998) 41.

[5] H. Jeppsen, H. Lenske, G. Schrieder et al., Phys.Lett. **B** (2005) (submitted).

[6] W. M. Bugg, G. T. Condo, E. L. Hart, H. O. Cohn, R. D. McCulloch, Phys. Rev. Lett. **31** 475 (1973).

[7] V. Ashford, M. E. Sainio, M. Sakitt, J. Skelly R. Debbe, W. Fickinger, R. Marino, and D. K. Robinson, Phys. Rev. C **30** 1080 (1984)

[8] S. Janouin, M.C. Lemaire, D. Garreta, P. Birien, G. Bruge, D.M. Drake, D. Legrand, B. Mayer, J. Pain, J.C. Peng, M. Berrada, J.P. Bocquet, E. Monnand, J. Mougey, P. Perrin, E. Aslanides, O. Bing, J. Lichtenstadt, A.I. Yavin, Nucl.Phys. **A451** (1986) 541.

[9] G. Bruge, A. Chaumeaux, P. Birien, D.M. Drake, D. Garreta, S. Janouin, D. Legrand, M.C. Lemaire, B. Mayer, J. Pain, M. Berrada, J.P. Bocquet, E. Monnand, J. Mougey, P. Perrin, E. Aslanides, O. Bing, J. Lichtenstadt, A.I. Yavin, J.C. Peng. 1986, Phys. Lett. **B169** (1986) 14.

[10] P. Lubinski, J. Jastrzebski, A. Groshculska, A. Stolnarz, A. Trzcinska, W. Kurcewicz, F.J. Hartmann, W. Schmid, T. von Egidy, J. Sklalski, R. Smolanczuk, S. Wycech, D. Hilscher, D. Polster, H. Rossner, Phys. Rev. Lett. **73** (1994) 3199.

[11] S. Wycech, J. Skalski, R. Smolanczuk, J. Dobaczewski, J.R. Rook, Phys. Rev. **C54** (1996) 1832.

[12] P.Kienle, NIMB **214** (2004) 193.

[13] I.A. Koop et al., Proc. EPAC 2002, Paris, p. 620.

[14] Proposal for the GSI Future Project, http://www.gsi.de.
[15] R. Krücken et al.,AIC Proposal for FAIR, submtitted to GSI Darmstadt, Jan. 2005.
[16] Letter of intent of the NUSTAR nuclear structure and astrophysics community at GSI, http://www.gsi.de/forschung/kp/kp2/nustar.html.
[17] H.-P. Duerr, E. Teller, Phys. Rev. **101** 494 (1956).
[18] Carlo Guaraldo, Nuovo Cim. **A102** (1989) 1137.
[19] J.A. Niskanen, Anthony M. Green, Nucl.Phys. **A404** (1983) 495.
[20] T. Suzuki, Nucl.Phys. **A444** (1985) 659.
[21] H. Heiselberg, A.S. Jensen, A. Miranda, G.C. Oades, J.M. Richard, Nucl.Phys. **A451** (1986) 562.
[22] S. Adachi, H.V. Von Geramb, Nucl.Phys. **A470** (1987) 461.
[23] Zhang Yu-shun, Liu Ji-feng, B. A. Robson, and Li Yang-guo, Phys.Rev. **C54** (1996) 332.
[24] A.M. Green, J.A. Niskanen, Quarks and Nuclei, ed. W. Weise, World Scientific, Singapore 1984.
[25] Tan Zhen-Qiangi and Gu Yun-Ting, J. Phys. G: Nucl. Part. Phys **15** (1989) 1699.
[26] G. Faldt and I. Hultage, J. Phys. G: Nucl. Phys. **4** (1978) 363.
[27] J. Cote, M. Lacombe, B. Loiseau, B. Moussallam and R. Vinh-Mau, Phys. Rev. Lett. **48** (1982) 1319.
[28] Charles J. Joachain, Quantum Collision Theory, North-Holland, 1984.
[29] F. Hofmann, H. Lenske, Phys. Rev. **C57** (1998) 2281.
[30] A. Akmal, V. R. Pandharipande and D. G. Ravenhall, PR **C58** 1804 (1998).
[31] H. Lenske, F. Hofmann, C.M. Keil, Rep.Prog.Nucl.Part.Phys. 46 (2002) 187.
[32] N. Tsoneva, H. Lenske, Phys. Lett. **B586** (2004) 213.
[33] G. Audi and A. H. Wapstra, Nucl. Phys. **A595** 409 (1995).
[34] M. Abramowitz and I. Stegun, Handbook of Mathematical Functions, Dover Publications Inc., New York, (1965).